A Model for Current Source Inverter fed Induction Motor

Piush Kumar & Vineeta Agarwal, Member IEEE

Abstract **- *A* model has been developed for self-commutated current source inverter (SCCSI) fed induction motor in synchronously rotating d-q reference frame using proportional regulators in speed and current loops. The steady-state parameters and slip regulator characteristics of the drive are determined experimentally. Transient as well as steady state performance is obtained by developing a computer programme in MATLAB. The analysis has been carried out for the different values of the speed and current controller parameters. It has been found that with an increase in speed controller parameter Kps, the stator current as well as torque developed by the motor both reduces but the transient time to reach the steady state condition increases. There is a large drop in dc link current with a change in speed. However, there is no effect on current and torque when current controller parameter K_{pi} changes, But, the stator voltage increases rapidly with an increase in K_{pi}. For the selected motor, controller parameter are obtained such that $K_{ps} \leq 20$ and $K_{pi} \leq 0.6$.**

Nomenclature

v_{as}, v_{bs}, v_{cs}	= Stator phase voltages
v_{qs}, v_{ds}	=Stator phase voltages in d-q reference frame
v_{qr}, v_{dr}	= Rotor phase voltages in d-q reference frame
i_a, i_b, i_c	= Inverter output currents
i_q, i_d	= Inverter output currents in d-q reference frame
i_{as}, i_{bs}, i_{cs}	= Stator currents
i_{qs}, i_{ds}	= Stator currents in d-q reference frame
i_{qr}, i_{dr}	= Rotor currents in d-q reference frame
i_{act}, i_{react}	= Active & reactive component of stator current
i_{ref}, i_c	= Reference current, Capacitor current
ω_e	= Electrical angular velocity of d-q axis
ω_r	= Electrical angular velocity of rotor
ω_{sl}	= Slip speed in rad/sec
ω_{slref}	= Slip speed command in rad/sec
T_e, T_l	= Electromagnetic torque and load torque
v_{dc}, i_{dc}	= Rectifier output voltage, DC link current
v_i	= Inverter input voltage
v_s, v_r	= Amplitude of stator & rotor voltage
r_s, r_r	= Stator & rotor resistance
l_s, l_r	= Stator & rotor self inductance
l_m	= Mutual inductance between stator and rotor
C	= Capacitance of each output capacitor
r_f, l_f	= DC link resistance & inductance
P	= Number of pole
J	= Moment of inertia of rotor 'Kg-m^2'
K_{ps}, K_{pi}	= Proportional gain of speed & current controller
K_3	= Constant parameter of dc link reference current
K_1, K_2,	= Slope of active and reactive component of slip regulator characteristics

I. INTRODUCTION

In many modern variable speed drives the demand is for a precise and continuous control of speed with long-term stability and good performance. The development of static converters for speed control application has led to an increased interest in the transient performance of the induction motor on a variable frequency supply [1]. The current source inverter (CSI) fed induction motor drive has emerged as a reliable, rugged and high performance adjustable ac drives [2]. In current source drives [3] torque is directly related to current rather than the voltage. Hence control of current ensures the direct and precise control of the electromagnetic torque and drive dynamics. Current-source variable frequency supplies are realized either with self commutated current source inverter (SCCSI) or with current-regulated inverter drives [4]. In order to facilitate the transient performance of the induction motor fed with (SCCSI), the general D-Q axis equations may be simplified by considering liberalization about a steady operating point [5]. Several techniques [6] have been suggested for analyzing and predicting the performance of induction motor on digital computer. The availability of number of software's packages for circuit simulation eg. SCEPTRE, ECAP, PCAP, PSPICE, CANDY, and MATLAB have reduced the problem of numerical solution of the time domain mathematical model to a relatively simple matter [7].

Current-source variable frequency supplies are realized either with self commutated current source inverter (SCCSI) or with current-regulated inverter drives [8]. This paper presents the dynamic behavior of SCCSI fed induction motor system using d-q equations representing the motor, inverter, and output capacitor mounted at the output of induction motor to meet out the reactive power demand. Incorporating proportional controller in speed and current loops carries out the simulation studies. Transient performance of the drive is obtained for different values of speed and current controller parameters.

II. CSIM FED DRIVE SYSTEM

Fig. 1 shows the schematic block diagram of the CSI fed induction motor drive system. The two control variables are 1) the input dc link current, i_{dc} and 2) inverter frequency ω_e. The input dc link current i_{dc} is controlled by a feedback current loop that controls the input voltage v_{dc}, obtained from the phase-controlled rectification of the three-phase ac supply. The control of v_{dc} is exercised by the firing angle controller, which controls the firing angles of the switches depending upon the value of current obtained from a current proportional controller. The time lag involved in the switching of the controlled rectifier forces the dc link to be provided with a large inductor to maintain a constant current and to provide protection during inverter and motor short-circuits.

The input to the current controller is the error between the reference current, i_{ref}, and dc link current, i_{dc}. It is to be noted that the inverter input current has to be positive, irrespective of the slip speed command signal. This is due to the facts that the controlled rectifier allows current only in one direction and that regeneration is handled by the reversal of the inverter input voltage (and hence, by the controller rectifier output voltage). The reversal of the input inverter voltage occurs because of the regeneration induced by the negative slip speed in the induction machine. The inverter input voltage reflects the machine phase voltage. The reversal of the voltage at the inverter input results in instantaneous increase in dc link current, which results in a negative current error. This negative current error produces a negative control voltage making the controlled rectifier produce a negative voltage across its output so as to oppose the inverter input voltage and their by maintain the dc link current at its commanded value. The reversal of the converter voltage is made possible by increasing the triggering-angle delay to the converter, resulting in the operation of the converter in its inverter mode. During this time, the converter output voltage is negative but its output current is positive, thus producing a negative power, implying that power from the machine is returned to the ac main via the dc link.

The speed control loop error generates the slip command signal ω_{sl} through a proportion speed controller and slip regulator. The slip regulator regulates the slip in safe operational bounds. Depending on the value of slip constant flux operation produces the dc reference current. Thus the slip speed command signal provides the inverter input-current command.

The slip command is added with the rotor speed signal to generate the frequency command. The frequency command also controls i_{dc} through an inner current loop to maintain a constant flux. The current i_c generated through a current/Hz function generator is compared with the reactive component of motor current. The resulting error controls the dc link current i_{dc}. At zero speed the developed torque is zero, but the current has a minimum value that corresponds to magnetizing current of motor. As the motor speed increases by ramping up the frequency command, the current i_{dc} also changes to maintain a constant flux. Thus, inner current loop provides the variable current source for feeding the inverter.

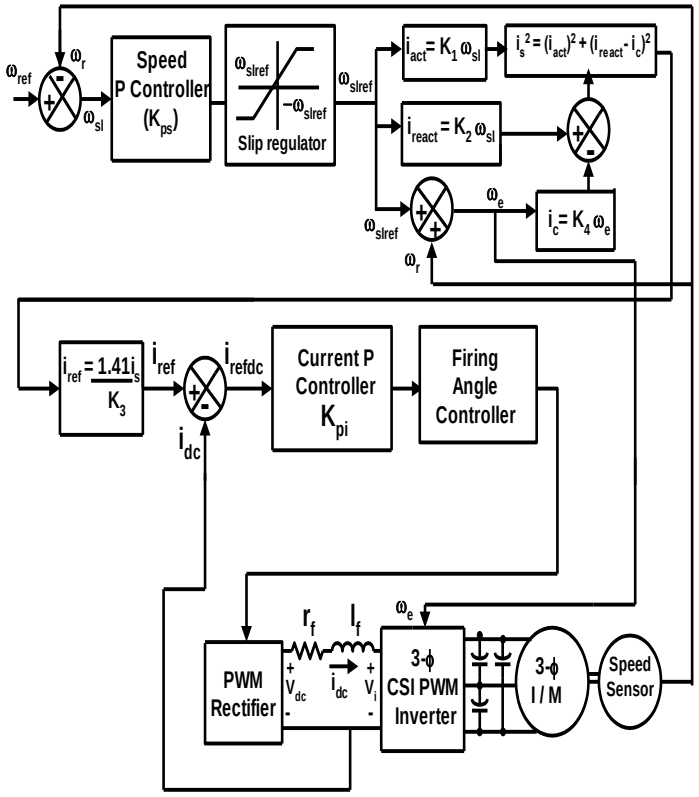

Fig. 1 Closed Loop Control Of Induction Motor fed by CSI

III. MODELING OF CSIM DRIVE SYSTEM

The composite inverter fed induction motor system has been modeled in different structures and cascaded together to obtain the overall performance of system.

a. Modeling of Induction Motor

The equations, which determine the behaviour of induction motor, are quite complex. A simplification of these equations for the purpose of analysis is possible using three particular cases of the generalized model of the induction motor in arbitrary reference frame namely: 1) stator reference frame model , 2) rotor reference frame model and 3) synchronously rotating reference frame. For this work the motor has been assumed to be ideal where space mmf and flux waves are sinusoidally distributed and saturation, hystersis and eddy currents are ignored. The motor voltages and currents are represented in a synchronously rotating d-q reference frame as

$$\begin{bmatrix} v_{qs} \\ v_{ds} \\ v_{qr} \\ v_{dr} \end{bmatrix} = \begin{bmatrix} r_s + pl_s & \omega_e l_s & pl_m & \omega_e l_m \\ -\omega_e l_s & r_s + pl_s & -\omega_e l_m & pl_m \\ pl_m & \omega_{sl} l_m & r_r + pl_r & \omega_{sl} l_r \\ -\omega_{sl} l_m & pl_m & -\omega_{sl} l_r & r_r + pl_r \end{bmatrix} \begin{bmatrix} i_{qs} \\ i_{ds} \\ i_{qr} \\ i_{dr} \end{bmatrix} \quad (1)$$

Solving (1), following model of induction motor is obtained

$$\begin{bmatrix} \dot{i}_{ds} \\ \dot{i}_{qs} \\ \dot{i}_{dr} \\ \dot{i}_{qr} \end{bmatrix} = \frac{1}{l_1} \begin{bmatrix} -r_s l_r & \omega_e l_1 + \omega_r l_m^2 & r_r l_m & \omega_r l_m l_r \\ -\left(\omega_e l_1 + \omega_r l_m^2\right) & -r_s l_r & \omega_r l_m l_r & r_r l_m \\ r_s l_m & -\omega_r l_m l_s & -r_r l_s & \omega_e l_1 - \omega_r l_s l_r \\ \omega_r l_s l_m & r_s l_m & -\left(\omega_e l_1 - \omega_r l_s l_r\right) & -r_r l_s \end{bmatrix} \begin{bmatrix} i_{ds} \\ i_{qs} \\ i_{dr} \\ i_{qr} \end{bmatrix} + \frac{1}{l_1} \begin{bmatrix} l_r & 0 & 0 & 0 \\ 0 & l_r & 0 & 0 \\ -l_m & 0 & 0 & 0 \\ 0 & -l_m & 0 & 0 \end{bmatrix} \begin{bmatrix} v_{ds} \\ v_{qs} \\ 0 \\ 0 \end{bmatrix} \quad (2)$$

Where $$l_1 = l_s l_r - l_m^2 \quad (3)$$

The machine and load torque are related as

$$Jp\omega_r = T_e - T_l \quad (4)$$

In (4) friction and windage losses are neglected. The electromagnetic torque, T_e and load torque, T_l is given by the following equations.

$$T_e = (3P/4) l_m \left(i_{qs} i_{dr} - i_{ds} i_{qr}\right) \quad (5)$$

$$T_l = T_L * (\omega_r / \omega_b) \quad (6)$$

The load torque in the present case is considered to be varying linearly with the speed.

b. Modeling of Capacitors

For the balanced condition, the equations related to the output capacitors can be expressed, in term of phase voltages as following:

$$i_a = 3Cpv_{as} + i_{as} \quad (7)$$

$$i_b = 3Cpv_{bs} + i_{bs} \quad (8)$$

$$i_c = 3Cpv_{cs} + i_{cs} \quad (9)$$

Transforming the inverter output currents i_a, i_b & i_c in a synchronously rotating d-q reference frame, following equations are obtained.

$$i_q = 3Cpv_{qs} + 3C\omega_e v_{ds} + i_{qs} \quad (10)$$

$$i_d = 3Cpv_{ds} - 3C\omega_e v_{qs} + i_{ds} \quad (11)$$

In CSI the inverter output current flow for 120° of each half cycle in the form of a rectangular wave. Their harmonic components are neglected on the assumptions that the drive system stability is primarily determined by the fundamental component of each variable. Thus, the inverter output currents considering only the fundamental component are achieved as below

$$i_q = (2\sqrt{3}/\pi) i_{dc}, \quad i_d = 0 \quad (12)$$

From equation (10) to (12) voltages in dq frame are obtained as

$$pv_{ds} = (1/3C)\left(-i_{ds} + 3C\omega_e v_{qs}\right) \quad (13)$$

$$pv_{qs} = (1/3C)\left((2\sqrt{2}/\pi) i_{dc} - 3C\omega_e v_{ds} - i_{qs}\right) \quad (14)$$

c. Modeling of DC Link

The dc link is expressed as

$$l_f pi_{dc} + r_f i_{dc} = v_{dc} - v_i \quad (15)$$

In (15) the ripple components of V_{dc} are neglected. Variable v_i is determined by the current injected from the inverter into induction motor. If inverter is assumed to be loss less, the inverter input voltage would be

$$v_i = (3\sqrt{3}/\pi) v_{qs} \quad (16)$$

d. Modeling of DC Link Current

Induction motor stator rms current is written as

$$i_s^2 = \left(i_{act}\right)^2 + \left(i_{react} - i_c\right)^2 \quad (17)$$

Where i_{act} & i_{react} are the functions of slip speed command and can be written as

$$i_{act} = K_1 \omega_{slref} \quad (18)$$

$$i_{react} = K_2 \omega_{slref} \quad (19)$$

The relationship between the stator rms current and dc reference current is

$$i_{ref} = (\sqrt{2}/K_3) i_s \quad (20)$$

e. Modeling of Frequency Command

The stator frequency is generated by the rotor speed loop and the slip speed command generated by the speed error between the reference and actual speed. The slip speed signal is limited by the fact that the operation of induction motor has

to be constrained with in high efficiency region of slip torque. The equations of the relevance are of following

$$\omega_{slref} = K_{ps}(\omega_{ref} - \omega_r) \quad (21)$$

$$\omega_e = \omega_r + \omega_{slref} \quad (22)$$

f. Modeling of Controlled Rectifier

The inverter current command is compared to the measured value of the inverter input current to produce an error signal which is amplified through a proportional current controller whose gain is K_{pi}. The output of current controller is limited to provide the safe operation of the converter during inversion. The output of current controller actuates the controlled rectifier to provide a proportional output voltage and to generate the inverter input current to match its command. The rectifier output voltage is given by

$$v_{dc} = K_{pi}(i_{ref} - i_{dc}) \quad (23)$$

IV. Results And Discussions

The test machine used in the work is a 3-phase, 400/440V, 50 Hz, 4 poles 7 Amps, induction motor. Its parameters are calculated by means of no load test, blocked rotor tests and load test. Slip regulator characteristics are drawn to calculate the constant parameters K_1 and K_2. Fig. 2 shows the plot between I_{act} and ω_{sl} and Fig. 3 shows the plot between I_{react} and ω_{sl} for V/f control operation of the drive. The slope of these slip regulator characteristic gives the value of K_1 and K_2 respectively.

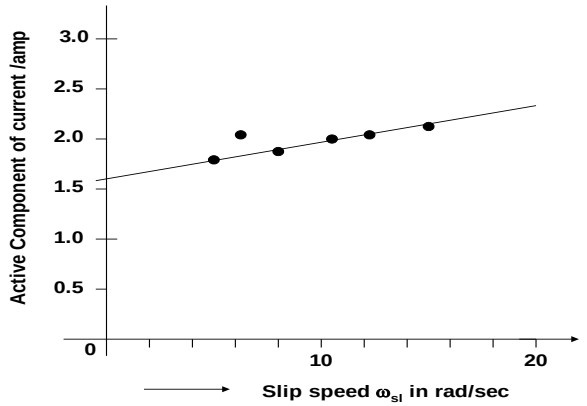

Fig. 2 Slip regulator characteristics (I_{act} vs ω_{sl} curve)

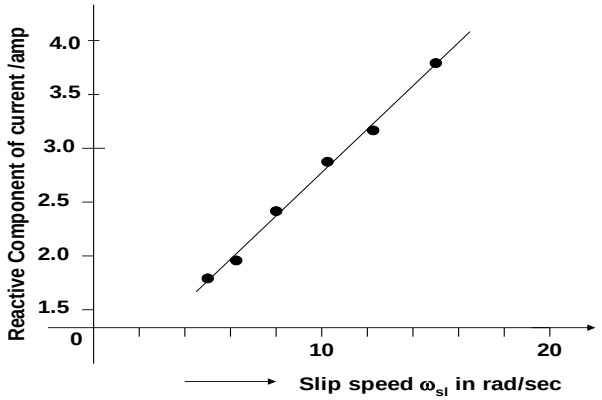

Fig. 3 Slip regulator characteristics (I_{react} vs ω_{sl} curve)

Different parameters of the motor are r_s = r_r 5.53 Ω/ph, l_s = l_r = 0.68 H, l_m=0.6503 H, $l_f = 0.05H$, $r_f = 3\Omega$, C = 28.22 μF, K_1 =0.0821 and K_2 0.2474..

The results of simulation are obtained for different values of speed and current controller parameters when motor speed is fixed at 1400 rpm (146.61 rad/sec). The steady state equation are obtained by putting all the derivative terms equal to zero in (1), (13) & (14). Once the DC link current required for an arbitrary speed and load torque is determined all the motor currents and the developed electromagnetic torque can be obtained. Fig. 4 shows the torque versus slip characteristics. Near the synchronous speed i.e. at low slips the torque is linear and is proportional to slip; beyond the maximum torque the torque is approximately inversely proportional to slip. Fig. 5 shows the rotor current characteristic for different value of dc link current .It shows that at unity slip the current taken by the motor is large as expected.

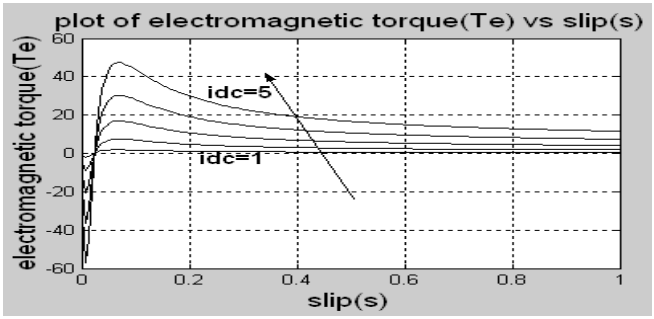

Fig. 4 Plot of electromagnetic torque (Te) vs slip(s)

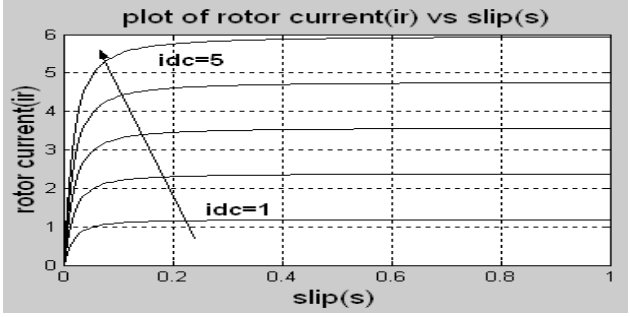

Fig. 5 Plot of rotor current (ir) vs slip(s)

Figures 6 shows the stator current waveforms for three different values of K_{ps}. Stator current may be divided into two time regimes: the transient period, and the steady state period during which the current is almost constant. It may be observed that the stator current during transient period is 1.4 times that in the steady state period for $K_{ps} = 20$. This ratio reduces to 1.3 for $K_{ps} = 25$ and 1.1 for $K_{ps} = 30$. The steady-state stator current reduces as the controller parameter K_{ps} is increased. This is due to the fact that resistance becomes increasingly significant at lower frequencies.

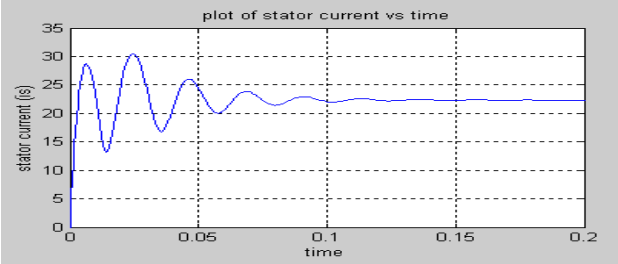

(a) K_{ps}= 20

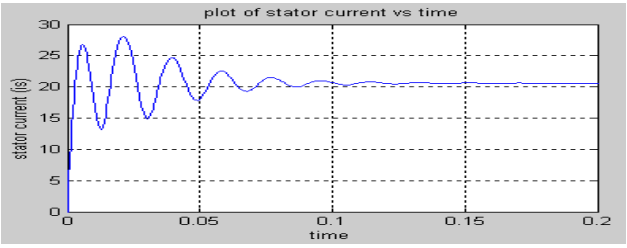

(b) K_{ps}=25

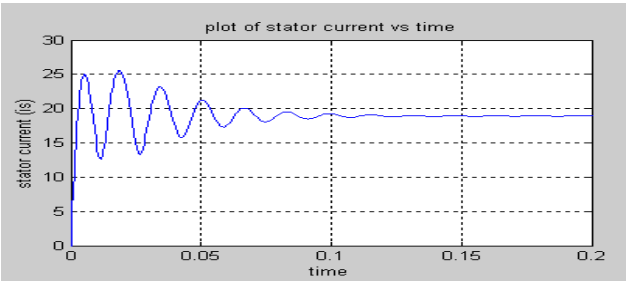

(c) K_{ps}=30

Fig. 6 Stator current waveforms for different value of K_{ps}

Figures 7 shows the DC link current waveforms for three different values of K_{ps}. Dc link current also reduces with an increase in controller parameter $K_{p.}$ due to the fact that resistance becomes increasingly significant at lower frequencies.

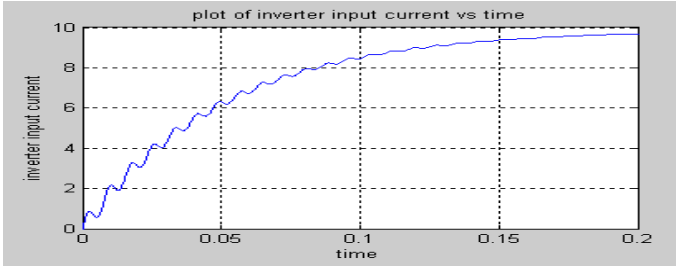

(a) K_{ps}= 20

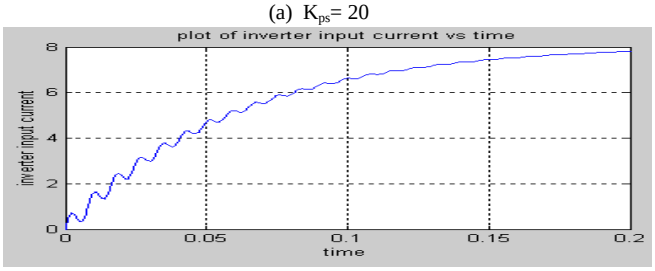

(b) K_{ps}= 25

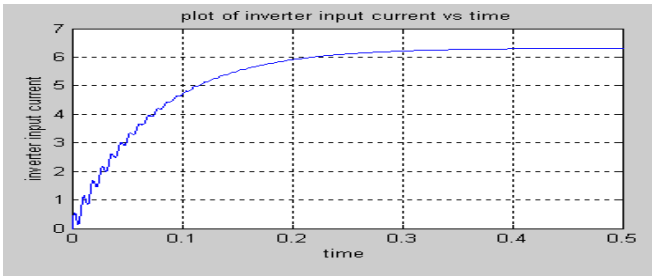

(c) K_{ps}= 30

Fig. 7 Inverter input dc link current for different value of K_{ps}

Figure 8 shows the stator voltage for three different values of K_{ps}. .The transient time to reach the steady state voltage increases as speed controller constant increases.

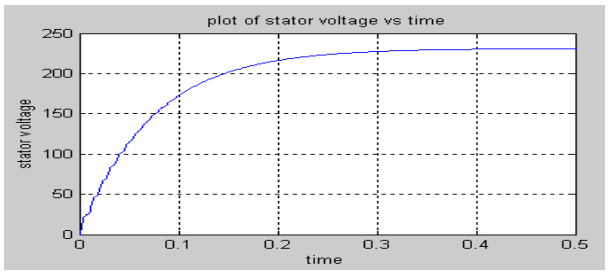

(a) K_{ps}=20

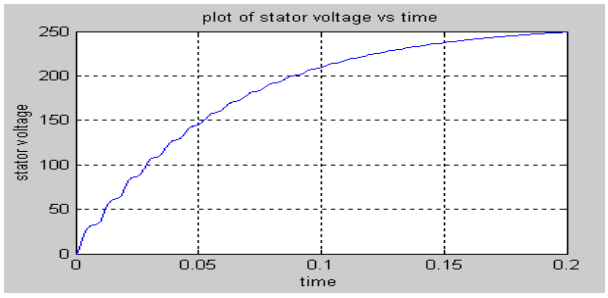

(b) K_{ps}=25

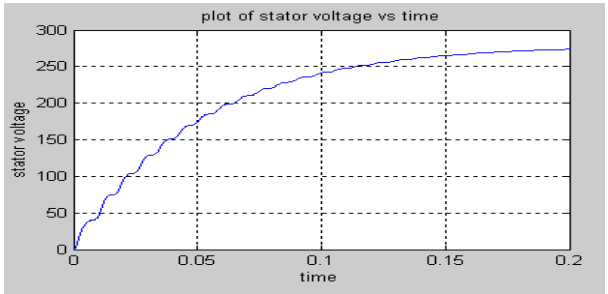

Fig. 9 shows the instantaneous torque. It is observed that torque developed is pulsating in the nature and it decreases as K_{ps} increases. This is caused by the reduction in gap flux at low frequency. The starting torque also decreases with the increases in speed controller constant

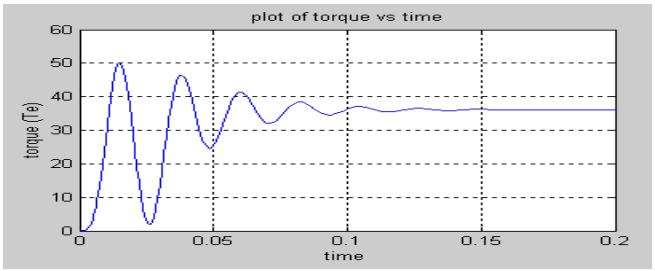

(a) K_{ps}=20

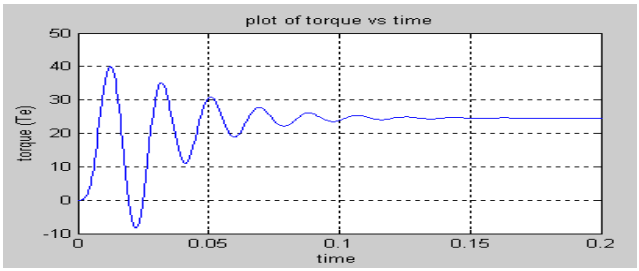

(b) K_{ps}=25

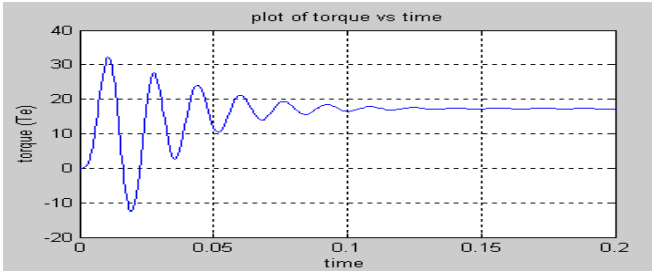

(c) K_{ps}= 30

Fig. 9 Instantaneous torque or different value of K_{ps}

Fig. 10 shows the rotor speed. The acceleration time for the motor to reach steady speed decrease with an increase in speed controller parameter the speed buildup shows oscillations about the synchronous speed.

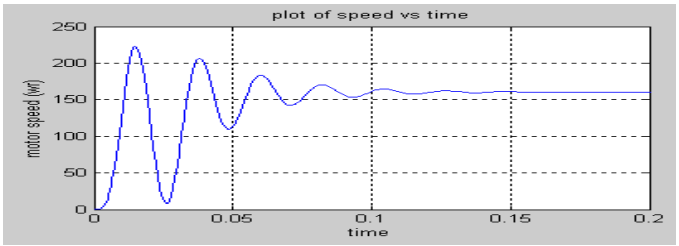

(a) K_{ps}=20

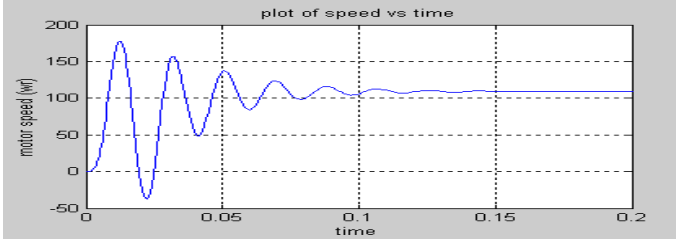

(b) K_{ps}=25

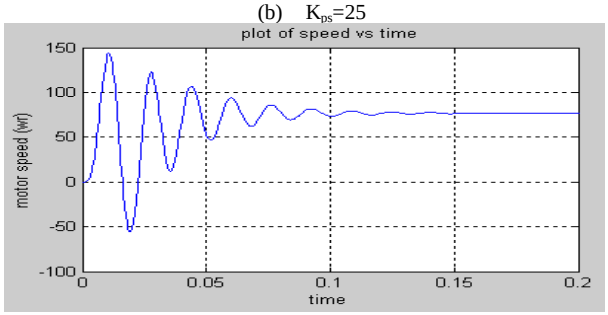

(c) K_{ps} = 30

Fig. 10 Rotor speed for different value of K_p

Fig. 11 and 12 show the stator current and torque for three different values of K_{pi} with constant K_{ps} = 20. It is observed that for both cases the behavior remain same for all values of K_{pi}

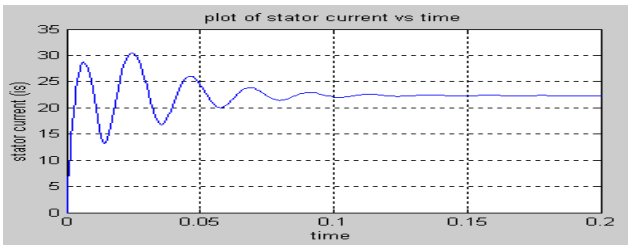

(a) K_{pi}= 0. 6

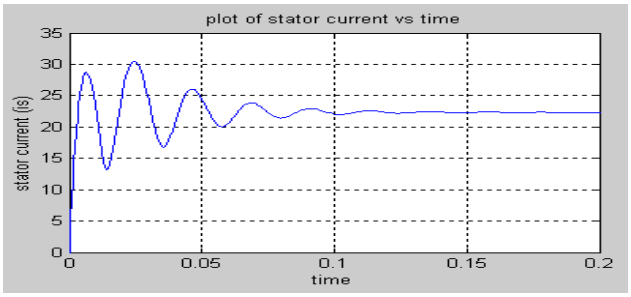

(b) K_{pi}= 0. 8

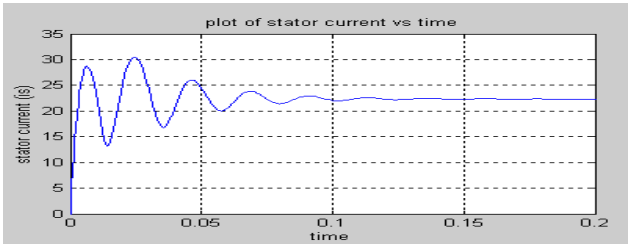

(c) K_{pi}=1

Fig. 11 Stator current for different values of K_{pi}.

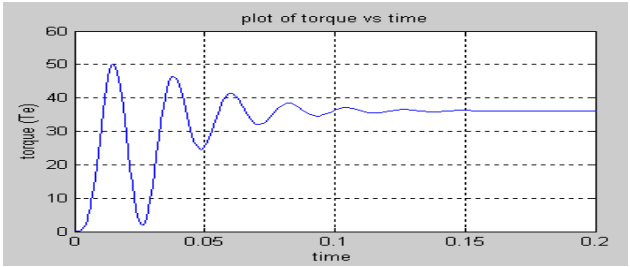

(a) K_{pi} = 0. 6

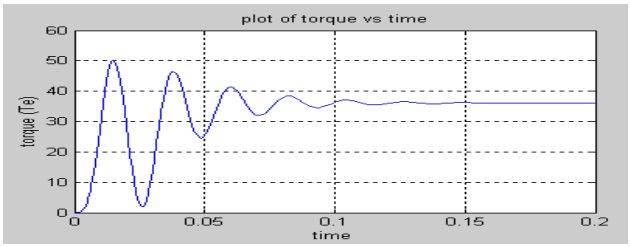

(b) K_{pi} = 0.8

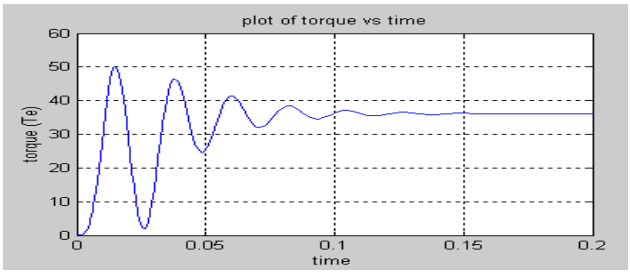

(c) K_{pi} = 1.0

Fig. 12 Instantaneous torque for K_{ps}=20

Figure 13 shows the stator voltage for three different values of K_{pi}. It is seen from the figures that the stator voltage increases rapidly with an increase in K_{pi}. Since the motor has to operate at the voltage below 440 volts, the maximum value of K_{pi} should be 0.6.

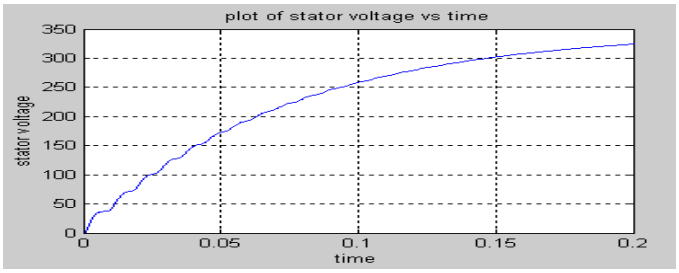

(a) K_{pi}=0.6

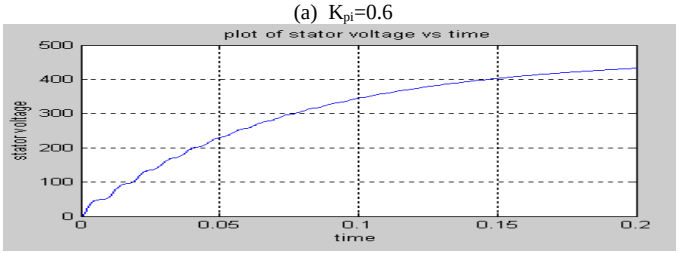

(b) K_{pi}=0.8

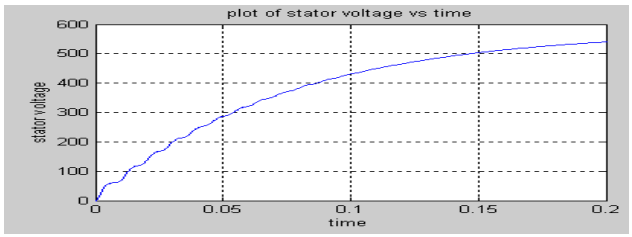

(c) K_{pi}= 1.0

Fig. 13 Stator voltage for different values of K_{pi}

Fig. 14 shows the dc link current. It may be observed that the input dc link current also increases with an increase in K_{pi}. Depending on the rating of switches in the rectifier, required value of K_{pi} may be selected. The steady state speed of 146.61 rad/sec corresponding to 1400 rpm is obtained for maximum value of $K_{ps} = 20$. So the parameters selected for CSI fed induction motor system should be such that $K_{ps} \leq 20$ and $K_{pi} \leq 0.6$ for the motor selected in the work.

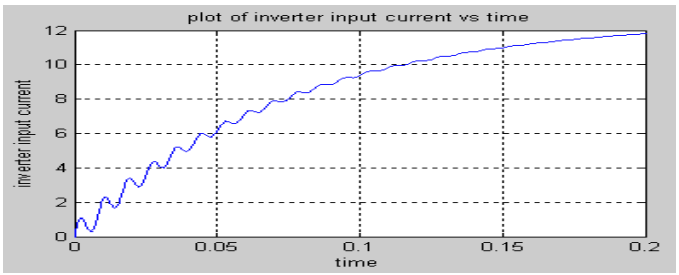

(a) K_{pi}=0.6

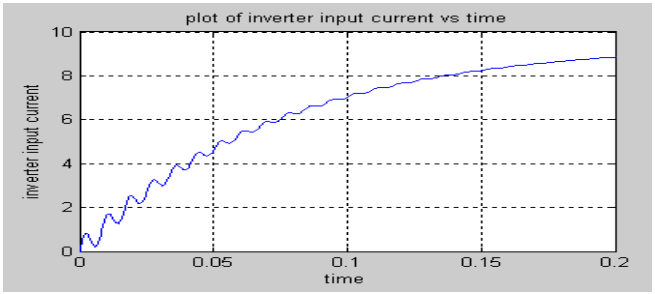

(b) K_{pi}= 0.8

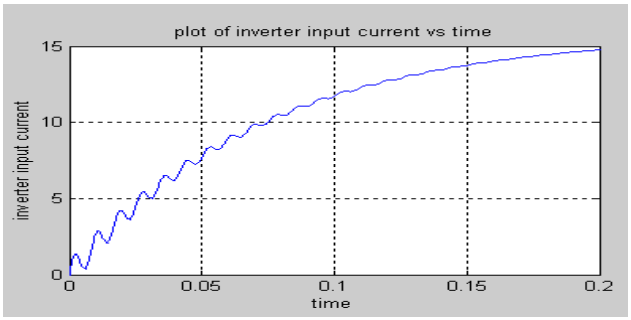

(c) K_{pi}=1

Fig. 14 Inverter input current for different values of K_{pi}

Fig. 15 shows the combined effect of parameters on speed transient response of the drive when reference speed is 146.61 rad/sec is settled for three different sets of controller parameters. It is observed from the figure, when parameters are as K_{Pi} =30 and K_{Ps} =0.5, the settling time of the drive is much larger as compared to the time when parameters are as K_{Pi} = 25 and K_{Ps} =0.45 and with parameter K_{Pi} = 20 and K_{Ps} = 0.6.

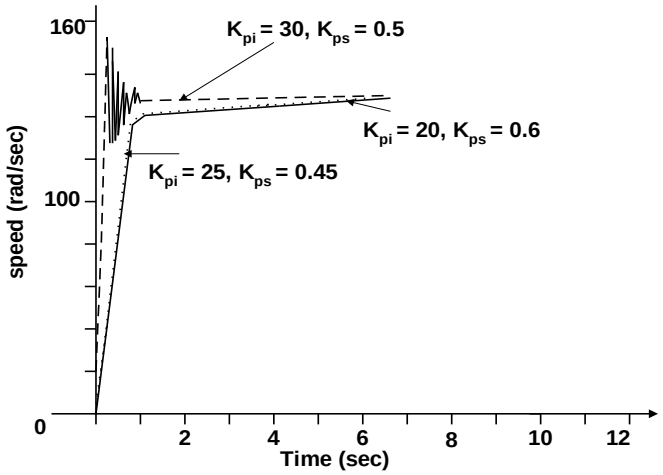

Fig. 15 Transient performance of the drive when speed

The change in reference dc link current during starting transient of the drive is shown in Fig. 16 when the speed is increased from 41.89 rad/sec to 146.61 rad/sec. It is observed that with K_{Pi} = 25 and K_{Ps} =0.45 or K_{Pi} = 20 and K_{Ps} = 0.6 the drop in current is less as compared to drop when the parameters are K_{Pi} =30 and K_{Ps} = 0.5. The same effect is observed in Fig. 18 when the drive speed is falling from 146.61 rad/sec to 41.89 rad/sec.

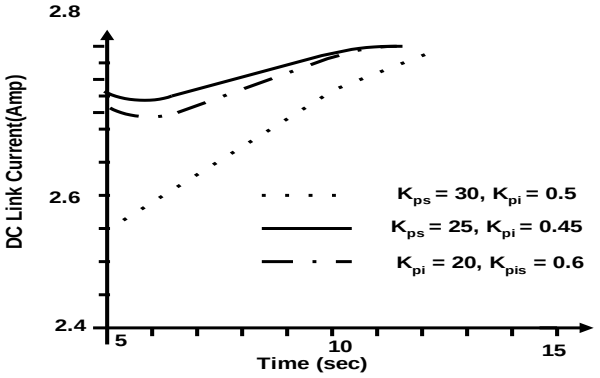

Fig. 16 Change in DC link for step change in reference speed for 41.89 rad/sec to 146.61 rad/sec .

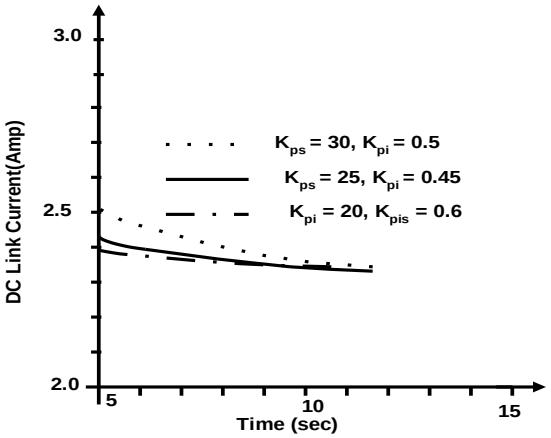

Fig. 17 Change in DC link for step change in reference speed for 146.61 rad/sec to 41.89 rad/sec.

V. CONCLUSIONS

Mathematical modeling of induction motor drive system using a self-commutated current source inverter (SCCSI) has been done in synchronously rotating d-q reference frame using proportional regulators in speed and current loops. A capacitor bank is mounted on the terminal of drive for maintaining better power factor at each operating condition of the drive. The steady-state parameters and slip regulator characteristics of the drive are determined experimentally. Transient performance is obtained by developing a computer programme in MATLAB. A number of observations have been made to analyze various waveforms. Motor has been loaded with rated load. Optimum value of controller parameters is determined for different values of K_{pi} and K_{ps} parameters. The load is varying linearly with speed.

REFERENCES

[1] T.A Lipo, Recent progress in the development of solid state ac motor drives, IEEE Trans Power Electronics, Vol. PE-3, pp 105-117, April 1988.

[2] B.K. Bose, Adjustable speed ac drives, A technology status review, Proc. IEEE, Vol. 70, pp. 116-135, Feb 1982.

[3] Ajit K Chattpadhyay, Current Source Inverter Fed Induction Motor Drives A state of the Art Research Review, JIE , Vol. 37, pp-34-46, 1991.

[4] S. Nonaka & Y. Neba, New GTO current source Inverter with pulse width modulation control Technique, IEEE Trans. Ind Appi. Vol. IA /22, pp. 666-672, July/Aug. 1986.

[5] M. Hombu, S. Ueda and A. Ueda, A current source GTO Inverter with sinusoidal inputs and outputs, IEEE Trans. on. Ind. Application. Vol. IA /23, pp. 247-255, March April 1987.

[6] M. K. Sang, Y. H. Woo, G. L Chang., Improved Self-tuning Fuzzy PID Controller for Speed Control of Induction Motor, IEEJ Trans. IA, Vol.124, No.7, 2004.

[7] M. Nasir Uddin, Hao Wen, Development of a Self-Tuned Neuro-Fuzzy Controller for Induction Motor Drives, Industry Application Conference, 2004, 39th IAS Annual Meeting Conference Record of the 2004 IEEE, Vol. 4, 3-7 Oct. 2004 Page(s): 2630-2636.

[8] Abdul Rahiman Beig, V. T. Ranganathan, A Novel CSI-Fed Induction Motor Drive, IEEE Trans. On Power Electronics, Vol.21, No.4, July 2006